Can surface pressure be used to remove atmospheric contributions from GRACE data with sufficient accuracy to recover hydrological signals?

Isabella Velicogna, ¹ John Wahr, ¹ and Huug Van den Dool²

Short title: GRACE ATMOSPHERIC MASS CORRECTION

¹Department of Physics and Cooperative Institute for Research in Environmental Science, University of Colorado, Boulder.

²Climate Prediction Center, National Centers for Environmental Prediction, Washington.

The GRACE satellite mission will resolve temporal variations in Abstract. gravity orders of magnitude more accurately and to considerably higher resolution than any existing satellite. Gravitational effects of atmospheric mass over land will be removed prior to estimating the gravitational field, using surface pressure fields generated global weather forecast centers. To recover the continental hydrological signal with an accuracy of 1 cm of equivalent water thickness down to scales of a few hundred km, atmospheric pressure must be known to an accuracy of 1 mbar or better. We estimate errors in analyzed pressure fields, and the impact of those errors on GRACE surface mass estimates, by comparing analyzed fields with barometric surface pressure measurements in the United States and north Africa/Arabian peninsula. We consider (1) the error in 30-day averages of the pressure field, significant because the final GRACE product will be a smoothed map averaged from measurements collected over 30-day intervals; and (2) the short-period error in the pressure fields, which would be aliased by GRACE orbital passes. Because the GRACE results will average surface mass over scales of several hundred km, we assess the pressure field accuracy averaged over those same spatial scales. The atmospheric error over the 30-day averaging period, which will map directly into GRACE data, is estimated to be generally < 0.5 mbar, and consequently will be adequate to remove the atmospheric contribution from GRACE hydrological estimates to sub-cm levels. However, the short-period error in the pressure field, which would alias into GRACE data, could potentially contribute as much as 1 cm of water thickness equivalent error. We also show that, given a sufficiently large density of barometers in a region, an accurate surface pressure field can be constructed from

surface pressure measurements alone.

1. Introduction

Most modern, high-precision geodetic measurements of time variable processes can benefit from accurate knowledge of atmospheric pressure. For example, precise space-based positioning methods (e.g. Global Positioning System (GPS), Very-Long-Baseline-Interferometry, Satellite Laser Ranging) require estimates of surface pressure and temperature to model the dry air contribution to the signal delay [e.g., Rocken et al., 1993]. The Earth's elastic response to loading by atmospheric pressure can cause vertical crustal displacements of up to 5 mm [e.g., Van Dam et al., 1994], and the direct attraction of the atmosphere can cause surface gravity signals of several µgals [Neibauer and Faller, 1992], both of which can contaminate estimates of tectonic motion. Accurate knowledge of the atmospheric mass distribution will be particularly important for the coming new generation of satellite gravity missions, and especially for GRACE (Gravity Recovery and Climate Experiment). Errors in the atmospheric contributions will likely be the largest source of error in GRACE measurements of time variable gravity over land, at scales of about 300 km and larger.

GRACE, under the joint sponsorship of NASA and the DLR (Deutsches Zentrum fur Luft und Raumfahrt), is scheduled for a 2001 launch with a nominal 5-year lifetime. GRACE will consist of 2 satellites in low-earth orbit (an initial altitude of 450-500 km) that range to each other across a few hundred km of separation using microwave phase measurements. Onboard GPS receivers will determine the position of each spacecraft in a geocentric reference frame. The geoid estimate will combine the GPS location

with ranging information and subtract out non-gravitational accelerations measured by onboard accelerometers. The resulting data will map the gravity field orders of magnitude more accurately, and to considerably higher spatial resolution, than any existing satellite.

GRACE will resolve temporal variations in gravity at length scales of a few hundred km and larger, and produce a complete global map once every 30 days. Temporal variations in gravity can be used to study a large number of problems in several disciplines, from monitoring changes in water, snow, and ice on land, to determining changes in ocean bottom pressure, to studying post-glacial rebound (PGR) of the solid earth. Comprehensive descriptions of these and other applications are given by *Dickey et al.* [1997] and *Wahr et al.* [1998].

Wahr et al. [1998] showed that GRACE has the potential to deliver 30-day estimates of surface mass at scales of a few hundred km and greater, with accuracies of better than 1 cm of equivalent water thickness over land and of a few tenths of a mbar or better in ocean bottom pressure. This conclusion was based on an analysis of synthetic geoid data and included the effects of contamination from other geophysical signals as well as the current best estimates of GRACE measurement errors. The authors found that the limiting error source for estimating changes in continental water storage at wavelengths greater than about 300 km will be contamination from the changing distribution of atmospheric mass. Satellite gravity measurements are incapable of separating the gravitational effects of the atmosphere from those of the underlying stored water. Analyzed atmospheric fields will be used to remove the effects

of the atmosphere over land from GRACE measurements, prior to constructing gravity solutions. But there will be errors in those fields which will then map into errors in GRACE residual hydrological estimates. In order to recover the continental hydrological signal with an accuracy of 1 cm of equivalent water thickness, the atmospheric pressure needs to be known to an accuracy of 1 mbar (i.e., the atmospheric mass needed to generate 1 mbar of pressure at the earth's surface is equivalent to the mass of 1 cm of water). Atmospheric errors are far less of a problem for GRACE estimates of ocean bottom pressure. Bottom pressure reflects the weight of the total overlying oceanic and atmospheric mass, and this total mass is also what determines the gravity signal. Thus there is no need to remove the effects of the atmosphere over the oceans from the GRACE measurements when inferring bottom pressure variability.

In their simulation of GRACE data, Wahr et al. [1998] assumed that the gravitational effects of atmospheric mass over land will be removed using surface pressure fields generated by one of the global weather forecast centers. They simulated errors in the pressure fields by taking the difference between 30 day averages of the pressure fields generated by the ECMWF (European Center for Medium Range Weather Forecasts) and those generated by the NCEP (National Centers for Environmental Prediction), and dividing that difference by $\sqrt{2}$. The factor of $\sqrt{2}$ was included under the assumption that the ECMWF and NCEP fields are about equally accurate and that errors in the fields are uncorrelated, so that the two fields contribute equally to the variance of the difference. To provide continuity with this previous analysis, when comparing the two analyzed fields in this paper we estimate the difference of the two

dividing by $\sqrt{2}$. For this reason, in the remainder of the paper we will describe the comparisons of two analyzed fields as rms error and refer to comparisons between measurements and analyzed fields (without the $\sqrt{2}$ factor) as rms difference. Note that in our analysis we assume that the observations have negligible error. In the discussion in section 5 we will show that this is a reasonable assumption.

There are two possible problems with Wahr et al.'s method of estimating the errors in the atmospheric corrections to GRACE. One is that the gravitational signal from the atmosphere is somewhat sensitive to how mass is distributed vertically through the atmospheric column. Surface pressure, on the other hand, depends only on the total mass in that column. Ignoring the effects of the vertical mass distribution is equivalent to assuming that all atmospheric mass variations occur in an infinitely thin layer at the Earth's surface. Swenson and Wahr [2000] assess this assumption by comparing gravity results computed using geopotential height fields to those computed using surface pressure fields. They concluded that the thin layer assumption introduces errors into GRACE estimates of surface mass with an rms of less than 1.0 mm of equivalent water thickness when averaged over all latitudes (though rms differences at some high latitude locations can be as large as 2-4 mm).

The other possible problem is that the ECMWF and NCEP pressure fields are likely to have errors in common, and these would not be included in Wahr et al.'s [1998] ECMWF/NCEP differences. It is thus desirable to find some alternative method of estimating errors in the pressure fields and their impact on GRACE surface mass estimates, including the effects of any common errors. This is the main purpose of our

paper.

We examine how well the surface pressure fields from the ECMWF and NCEP/NCAR (National Center for Atmospheric Research) Reanalysis models reproduce barometric measurements of surface pressure in two regions: the United States and north Africa/Arabian peninsula (Figure 1). Both regions have large areas of low and high topographic relief, but whereas the United States has numerous high-quality barometric observations, pressure measurements in north Africa/Arabian peninsula are sparser, have more temporal gaps and more and larger outliers. We have considered Egypt and the Arabian peninsula because both have been proposed as focus regions for verification of GRACE accuracy, due to their extremely low precipitation and relatively simple hydrologic systems. The United States can be considered representative of the best-case scenario for observational constraints of surface pressure, while the distribution of pressure measurements in north Africa/Arabian peninsula is probably more typical of the global coverage. We base much of our comparison on the assumption that errors in the barometric measurements are much smaller than errors in the analyzed pressure fields. Most of the pressure measurements used in our comparison were assimilated in the course of the modeling and analysis procedure, so that the effects of measurement errors may be common to both pressure fields, and short scale variability that is spatially aliased by the measurements could be aliased into both. In section 5 of the paper we will carefully examine this assumption.

A secondary objective of this paper is to verify whether or not the surface pressure field over a given region can be constructed accurately from surface pressure Figure 1

measurements alone. Is it feasible to expect that a network of barometers could deliver atmospheric corrections to GRACE that might be better than those obtainable with ECMWF or NCEP/NCAR gridded fields? For this issue we focus specifically on the United States.

When estimating the effects of atmospheric pressure errors on GRACE, it is useful to separate those errors into two components: (1) the pressure errors averaged over 30-day intervals, which are relevant because GRACE will average the measurements collected over 30-day periods to produce geoid maps; and (2) short-period pressure errors, which will be undersampled by GRACE orbital passes and hence will not average out entirely in the GRACE geoid maps. In this paper we will consider both components of the final error.

2. Preliminaries

To motivate this analysis we first describe the characteristics of GRACE data, and how these data will likely be used to estimate surface mass variability. We also discuss here the data sets used in this paper.

2.1. Spatial averaging

The Earth's global gravity field is commonly described in terms of the shape of the geoid: i.e., the equipotential surface corresponding to mean sea level over the oceans.

The geoid can be expanded in a spherical harmonic representation as:

$$N(\theta, \phi) = a \sum_{l=0}^{\infty} \sum_{m=-l}^{l} \tilde{P}_{lm}(\cos \theta) \{ C_{lm} \cos m\phi + S_{lm} \sin m\phi \}, \tag{1}$$

where a is the Earth's radius, θ and ϕ are colatitude and east longitude, C_{lm} and S_{lm} are dimensionless coefficients, and \tilde{P}_{lm} are the normalized associated Legendre functions [e.g. Chao and Gross, 1987].

Once every 30 days GRACE will provide a geoid model (i.e., numerical values for C_{lm} and S_{lm}) up to degree and order (l and m) of about 100, corresponding to spatial scales (i.e. half-wavelengths) of about 200 km and greater. Changes in C_{lm} and S_{lm} are related to changes in the Earth's density distribution, $\Delta \rho(r, \theta, \phi)$ via [Wahr et al., 1998]:

$$\left\{ \begin{array}{l} \Delta C_{lm} \\ \Delta S_{lm} \end{array} \right\} = \frac{3}{4\pi a \rho_{ave} (2l+1)} \int \Delta \rho(r,\theta,\phi) \, \tilde{P}_{lm}(\cos\theta) \\ \mathbf{x} \left(\frac{r}{a}\right)^{l+2} \left\{ \begin{array}{l} \cos m\phi \\ \sin m\phi \end{array} \right\} \sin\theta \, d\theta \, d\phi \, dr$$
(2)

where ρ_{ave} (=5517 kg/m³) is the average density of the Earth, and ΔC_{lm} and ΔS_{lm} are changes in the spherical harmonic coefficients of the geoid.

Suppose that $\Delta \rho$ is concentrated in a thin layer of thickness H at the Earth's surface, which should be thick enough to include those portions of the atmosphere, oceans, ice caps, and below-ground water storage with significant mass fluctuations. H thus approximately corresponds to the thickness of the atmosphere and is of the order of 10-15 km. Note that because of the radial integral in (2), GRACE will be

unable to resolve mass anomalies at different radial positions, and so will be incapable of distinguishing between water on the surface, in the soil, or in subsoil layers, and will also be unable to discriminate between water, snow, ice or atmospheric mass variations. This is the reason that variations in atmospheric mass will contaminate estimates of continental water storage (if the latter are to be measured by GRACE and the former cannot be accurately eliminated).

Because H is much less than the shortest spatial scale provided by GRACE, the factor $(r/a)^{l+2}$ in (2) can be approximated as 1, so that ΔC_{lm} and ΔS_{lm} can be related to the change in surface mass density $\Delta \sigma(\theta, \phi) = \int_{thin\ layer} \Delta \rho(r, \theta, \phi) dr$. That relation can be inverted to give $\Delta \sigma$ in terms of the ΔC_{lm} and ΔS_{lm} 's (see Wahr et al. [1998]'s equation (14)).

In principle, an estimate of $\Delta \sigma$ at any individual point (θ, ϕ) requires knowledge of the ΔC_{lm} and ΔS_{lm} 's at all wavelengths. But not only will GRACE deliver 30-day coefficients only up to about l=100, but the accuracy of those coefficients will decrease rapidly with increasing l, so that point-wise estimates of $\Delta \sigma$ would be too inaccurate to be useful. Instead, what GRACE will be able to deliver accurately will be spatial averages of surface mass over regions of a few hundred kilometers in scale. For this paper, we will follow $Wahr\ et\ al.\ [1998]$, and construct the spatial average:

$$\overline{\Delta\sigma}(\theta,\phi) = \int \Delta\sigma(\theta',\phi') W(\gamma) \sin\theta' d\theta' d\phi'$$
(3)

where γ is the angular distance between the two points (θ, ϕ) and (θ', ϕ') , and $W(\gamma)$ is the normalized gaussian function developed by Jekeli [1981] and depicted in Figure 2:

Figure 2

$$W(\gamma) = \frac{b}{2\pi} \frac{\exp[-b(1-\cos\gamma)]}{1 - e^{-2b}}.$$
 (4)

where

$$b = \frac{\ln(2)}{(1 - \cos(r_W/a))} \tag{5}$$

Here W has been normalized so that its global integral is 1, and r_W is the distance along the Earth's surface at which $W(\gamma)$ has decreased to half the value it had at $\gamma = 0$. We will refer to r_W as the averaging radius. GRACE measurements will deliver accurate estimates of $\overline{\Delta \sigma}$ for values of r_W of a few hundred kilometers and greater.

2.2. Data

The main purpose of this paper is to estimate how accurately the atmospheric contribution to the time-variable geoid can be determined. To do this we compare analyzed surface pressure fields from ECMWF and NCEP/NCAR with surface pressure observations. We also examine the possibility of using barometric measurements alone, without any input from the pressure fields generated by global circulation models, to reproduce the surface pressure fields. To examine each of these issues, we use 6-hourly gridded global surface pressure fields from 1998, 1460 fields in all. We use NCEP/NCAR Reanalysis data, sampled on $2.5^{\circ} \times 2.5^{\circ}$ global grids [Kalnay et al., 1996], and ECMWF analysis data, sampled on a global gaussian grid spacing of 1.125° [ECMWF, 1995]. Both centers have an analysis at higher resolution; however these data sets were not available to us and generally are not available to outside users.

The analyzed pressure fields were compared with 6-hourly barometric surface

pressure measurements from the NCEP global surface observations data set. NCEP collects these data on an operational basis to serve as constraints on environmental models, and some quality control is applied. A significant problem arises in that many of these same data are also assimilated into NCEP and ECMWF global circulation models, and so the models and the observations we are comparing here are not fully independent. Consequently it is difficult to make a clear estimate of the true error in the models. But as we will demonstrate, it is possible to assign upper and lower bounds to the error. The NCEP observational data sets include information about barometer elevations, but the barometer measurements are subject to transcription and other errors which must be addressed. We used a semivariance analysis [Davis 1986] in which the semivariance S^2 of all measurements spaced six hours apart was estimated from the data at a given site. Then all measurements which differed from the temporally closest measurements at > 4S (99.95% confidence) were considered outliers in the pressure measurement time series and removed from the comparisons (Figure 3).

Figure 3

To compare the observed and analyzed surface pressure fields we also need surface temperature and topography data for the analyzed field. For this we use ECMWF and NCEP/NCAR 6-hourly temperature and topography fields sampled on the same grid as the corresponding analyzed surface pressure fields. All data sets used in this paper were provided by the NCAR DSS (Data Support Section) archive.

As already noted, the analyzed ECMWF and NCEP/NCAR pressure fields are not independent of the surface pressure observations we will compare them with, because most of the available pressure observations were assimilated into the models when constructing the analyzed fields (96% of the observations available in the United states were assimilated and 82% in north Africa/Arabian peninsula). Roughly speaking the 3-D multivariate atmospheric analyses made by ECMWF and NCEP incorporate observations as:

$$Analysis(t) = \beta * observation(t \pm 3hours) + (1 - \beta) * guess$$

where t is time and the guess is a 6 hour forecast initialized using a previous analysis at (t-6hrs). β and $(1-\beta)$ can be interpreted as the inverse square of the assumed error in observations and the forecast respectively. Because different observations have different assumed errors (e.g., radiosondes are supposed to be more accurate than satellite data), the value of β is not quite unambiguous. Most centers appear to have a 'global' β in the 0.3-0.5 range. However, the real purpose of assimilating observations into these analyses is not necessarily to better describe the current state of the atmosphere, but to serve as initial conditions for 10 day forecasts. Consequently, the guess field is weighted as much as, or more than the observation to avoid initial "shocks" (i.e., unstable oscillations) when making a forecast.

3. Calculation of the atmospheric surface pressure error

We estimate the error in analyzed surface pressure fields from ECMWF Analysis and NCEP/NCAR Reanalysis by comparing with surface pressure observations. The GRACE final error will be some combination of the mean error over the 30-day averaging period and the error from unmodeled high frequency pressure variations that are aliased by orbital undersampling. The 30-day pressure errors will map directly into the 30-day

GRACE averages. But the aliasing error will depend in a complicated manner on the GRACE orbital configuration, and cannot be predicted without detailed orbital simulations.

We will examine two different estimates of the error: (1) the rms difference between model and observations averaged over twelve consecutive 30-day periods during 1998; and (2) the 6 hourly rms difference (i.e., without time averaging) over that same year. Because the GRACE observations will spatially average the mass variations, we use the normalized averaging function W in equation (4) to spatially average the error. The 6 hourly rms difference does not map directly into an error in the GRACE estimate of changes in surface mass because a high frequency error in one region will not necessarily be aliased into a 30-day value over only that same region. Still, the 6 hourly rms differences do provide some measure of the amplitude of the aliased signal. We expect our 6-hourly comparisons may over-estimate the total error, since the process of constructing 30-day GRACE values will presumably smooth out some fraction of the high frequency contributions.

3.1. Interpolation of analyzed pressure to barometer locations

The analyzed pressure fields are defined on a regular discretization over the globe whereas the barometer locations are irregularly spaced. For this reason we horizontally interpolate the analyzed pressure fields to the barometer locations (or vice versa) prior to calculating the rms difference between the two. For these comparisons we will consider interpolations going both directions (i.e., (1) from the analyzed field to the barometer

locations, and (2) from the observation field to the model grid point). To simplify the description of how the interpolation is performed, we describe here just the interpolation from analyzed pressure fields to the barometer locations. The interpolation going in the opposite direction is completely analogous however.

Because the barometer is generally at a different elevation than are the nearby model grid points, the analyzed surface pressure is first adjusted to the elevation of the barometer prior to horizontal interpolation. For a given location, we assume the relationship between pressure at two different elevations, h_1 and h_2 , corresponds to that of a dry, hydrostatic atmosphere and a uniform lapse rate of $0.0065 \,^{\circ}\text{K m}^{-1}$ [Haurwitz, 1941]:

$$p_m(h_2) = p_m(h_1) \left(1 + \frac{0.0065 \mid h_1 - h_2 \mid}{T_1} \right)^{\frac{sign(h_1 - h_2)}{\alpha}}$$
(6)

where $p_m(h_i)$ is the analyzed pressure at elevation h_i , T_1 is the surface temperature at height h_1 in ${}^{\circ}K$, $\alpha = 0.0065R_d/g$, where g is the gravitational acceleration and R_d (= 287 J K⁻¹ kg⁻¹) is the gas constant for dry air.

We first reduce the pressure from the four nearest grid points of the analyzed field, A, B, C and D, from their elevations (h_A, h_B, h_C, h_D) to the elevation h_Z of the barometer location Z using (6). Then we calculate the 2-dimensional Lagrange polynomial interpolation of the four reduced values of analyzed surface pressure to the barometer location Z.

3.2. The gaussian average of rms surface pressure differences

To simulate the signal delivered by GRACE, we calculate spatial averages using the gaussian weighting function described in (4) and shown in Figure 2. We approximate the gaussian average $\overline{F}_G(P)$, about the point P, of a function f defined only at a set of N discrete points, as:

$$\overline{F}_G(P) = \frac{\sum_{i=1}^{N} f_i W(\gamma_i)}{\sum_{i=1}^{N} W(\gamma_i)}$$
(7)

where P is the center location of the gaussian defined by $W(\gamma)$ (see equation 4), γ_i is the angular distance between P and the sampled point i, $W(\gamma_i)$ is the value of the weighting function at the point i where f is defined, and N is the total number of discrete samples of f. In our case, f_i will be the difference between two different surface pressure values at the location i. This difference is most often between the observed pressure and either the ECMWF or NCEP/NCAR analyzed pressure field, interpolated to the location of the i'th barometer. For comparisons of the ECMWF and NCEP/NCAR analyzed pressure fields with each other, the difference is calculated after reduction and interpolation of the NCEP/NCAR analyzed field to the ECMWF grid points. Once we have computed time series of $\overline{F}_G(P)$ for both pressure fields at a point P, we remove the yearly means from those time series and compute the rms of the residual difference between the two. The rms value is an estimate of the size of the pressure field difference, spatially averaged about the location P. We evaluate the rms difference of gaussian averages for values of P evenly spaced at every 0.2° interval

of latitude and longitude over the region of interest, using a 250-km gaussian radius. Note that near the edges of the map, differences are in general slightly larger because the comparison does not include points outside the map area. We evaluate this rms error both for 30-day averages of the pressure differences and for the original 6-hourly values (see section 1). We assume a gaussian averaging radius (r_W in (4)) of 250 km, since that is the order of the smallest r_W over which GRACE will provide useful hydrological estimates. We calculate the rms difference between analyzed pressure fields and barometric measurements only in continental regions, since our focus here is on atmospheric contamination of GRACE hydrological estimates. Oceanic surface pressure errors will not impact the GRACE surface mass estimates, for reasons discussed in the introduction.

4. Results

4.1. Rms differences for the 30-day averages

Sample time series of observed data and interpolated analyzed fields are shown in Figure 4 for two sites in the United States, one in a low relief area and one in a mountainous region. The Figure shows a good agreement between the time series. The rms values of 30-day averages of these differences, computed after removing the temporal mean, are contoured for the United States in Figures 5a and 5b for ECMWF and NCEP/NCAR analyzed fields respectively. The rms difference is generally < 0.2 mbar in low-relief areas for both ECMWF and NCEP/NCAR data, and larger in areas

Figure 4

Figures 5a

5b

of high elevation: up to 0.35 mbar for NCEP/NCAR and slightly more for ECMWF. Larger rms is expected in association with high elevation because the coarse spatial resolution of the models (> 100 km) is inadequate to resolve complex orographic effects on temperature, humidity and pressure, and because equation (6) could be problematic for large vertical adjustments.

Figures 5c and 5d depict the rms differences for the 30-day averages over north Africa/Arabian peninsula. In this area the distribution of barometers is much less dense than over the U.S. and the observations often contain large gaps. This partially explains the rms > 0.3 mbar in low-relief southern Egypt. Otherwise, differences in low-lying areas are generally ~ 0.2 mbar for both ECMWF and NCEP/NCAR, except in a few locations where particularly sparse observations yield larger rms around 0.3 mbar. However in the mountainous regions of the Turkish-Iranian Plateau, where the observation sites are denser, the rms difference for ECMWF exceeds 0.4 mbar, with values of up to ~ 0.7 mbar around the Caspian Sea. In the same area the rms difference for NCEP/NCAR is ~ 0.3 mbar and > 0.4 near the Caspian Sea.

One of the problems with the comparison depicted in Figure (5) is that the ECMWF and NCEP/NCAR analyzed pressure fields are not independent of the surface pressure observations we are comparing them with. By calculating the rms difference at the barometer location, we are comparing to assimilated observations at the point where they have been assimilated. Consequently the comparison does not necessary reflect the accuracy of the analyzed fields where there are no nearby observations to assimilate. Hence we would expect the rms difference calculated at the barometer locations to

Figures 5c

5d

approximate a lower bound estimate of the error in the analyzed fields.

To estimate the error in the analyzed pressure fields where there are no assimilated barometric measurements, we also interpolated surface pressure observations to the grid discretization of the analyzed fields. The analyzed fields are "interpolating" the pressure measurements using the governing equations of atmospheric circulation and with the aid of other datasets (including radiosonde profiles and wind velocities, which are a sensitive indicator of the pressure gradient). Hence the analyzed fields should produce a very different (and, ideally, much more accurate) "interpolation" of the assimilated barometric measurements than the simple Lagrange polynomial we have used here. Consequently, by interpolating barometric observations to the model grid and then comparing, we should get an upper-bound estimate of the error in the analyzed fields consisting of the true error plus differences due to sampling limitations and interpolation error. The interpolation was done in essentially the same manner as that from the model grid to the barometer locations, except that the temperature at each barometer site (needed for the vertical reduction in equation (6)) was first interpolated and reduced from the analyzed fields.

There are other reasons why this comparison is expected to overestimate the true error in the analyzed field. For example, there are gaps in the observed time series (whereas the analyzed field time series were complete). Consequently, if at time t one (or more) of the 4 nearest barometers had no pressure measurement, the next nearest barometer was used, potentially resulting in interpolation from a very large distance.

Moreover, any errors in the reduction and interpolation that were bias errors going from

the model grid to the barometers (and hence are removed by removing the means) are not necessarily bias errors in the interpolation of barometers to the model grid, because different stations are used for the interpolation at different times during the year.

Hence, by interpolating in both directions we are able to approximate both a lower bound and an upper bound estimate of error. If we assume that the observations are error-free (see the discussion in section 5 below), we can conclude that the true error lies between these 2 estimates. Figures 6a-6b show the rms difference evaluated at the model discretization for the 30-day averages of the ECMWF and NCEP/NCAR analyzed field, respectively, in the United States. Comparing these figures with Figures 5a-5b we note that values in Figures 6a-6b are slightly larger but mainly < 0.2 mbar in the low-lying areas for both ECMWF and NCEP/NCAR Reanalysis. Also in the Rocky Mountain region the rms difference in Figures 6a-6b is generally only slightly larger than in Figure 5a-5b. However in the upper Great Lakes region the rms difference is larger for the comparison at the model grid points (> 0.2 mbar) than for the comparison at the barometer location ($\sim 0.1 \text{ mbar}$). Note that as we are not considering barometric measurements over the ocean, the rms difference is larger near the coastlines, for the same reason that it is larger at the margin of the map. For north Africa/Arabian peninsula the results of the comparison at the model grid points are summarized by a map average in Table 1. These values can be compared with the map averages for comparisons at the barometer locations. The map averages for comparisons at the model discretization are 40% - 90% larger.

The rms errors (see section 1) between 30-day averages of ECMWF and of

Figures 6a

6b

Table 1

NCEP/NCAR are shown in Figures 7a and 7c. In the United States (Figure 7a) the rms errors are low, < 0.1 mbar, in low-relief areas. At higher elevations the rms is larger (> 0.1 mbar) and correlated with elevation. Note that the rms errors from the analyzed fields (Figure 7a) are substantially less than the rms differences between the models and observations (Figures 5a-5b,6a-6b), indicating either that the errors in the ECMWF and NCEP/NCAR analyzed fields are not entirely independent, or that there are non-negligible errors in the barometer observations. Also, the altitude difference between grids is less than between grid and observations, so part of the reduction of error could result from a decreased contribution of error introduced by vertical adjustment using equation (6). However we will show in section 4.3 that this contribution is unlikely to exceed a few tenths of a mbar. Figure 7c shows the rms error from the 2 models for north Africa/Arabian peninsula region. The rms errors are quite low throughout the entire area and are, again, slightly larger in the Turkish-Iranian Plateau.

4.2. Rms differences for the 6-hourly values

The maps in Figures 8a, 8b, 8c and 8d show rms differences between the 6-hourly values of the barometric measurements and the analyzed fields at the barometer locations with no time averaging, using a 250-km gaussian average. These maps provide information about the short-period errors (i.e., semidiurnal, diurnal,...< 60 days) that will alias into the GRACE 30-day estimates, in addition to the long-period (≥ 60 days) that will map directly into GRACE estimates of surface mass change. This rms is significantly larger than the rms of the 30-day averages shown in Figures 5a—5d. In

Figures 7a

7c

Figures 8a

8b

8c

8d

the United States, low-relief regions typically have rms < 0.5 mbar for both ECMWF and NCEP/NCAR data (Figures 8a-8b). Larger rms differences in the west, up to 0.8 mbar, appear to be generally correlated with high topographic relief—particularly in the case of the NCEP/NCAR pressure field. If we look at the rms difference between the analyzed fields and observations interpolated to the model grid points (Figures 6c-6d), we find that the values are larger than in Figures 8a-8b but that they are generally < 1 mbar, except in the Great Lakes region. Figure 7b shows rms error of the 6-hourly NCEP/NCAR and ECMWF data. The rms is < 0.4 mbar at low elevations and larger

(~ 0.5 mbar) in the Rocky Mountain region. Figures 8c–8d depict rms ~ 0.5 mbar in the Arabian peninsula for the NCEP/NCAR pressure field, and slightly larger values for ECMWF. Large rms (> 1 mbar) in the south probably results from the sparse barometer distribution and gaps in the timeseries. Table 1 gives map averages for the comparisons at the model grid points, which are 20% -50% larger than those of the comparisons at the barometer locations. The rms error of the 6-hourly fields of the two models (Figure 7d) is generally small (~ 0.4 mbar in the Arabian peninsula and $\lesssim 0.6$ mbar in north Africa), except for the Turkish-Iranian Plateau where the rms is ~ 0.7 mbar.

Figure 7d

4.3. Error sensitivity analysis

We expect that some fraction of the differences we have found between the observations and the analyzed fields is due to interpolation error, which will tend to cause our rms differences to over-estimate the true error in the analyzed fields. In this

Figures 6c

6d

Figure 7b

section, we discuss some of the possible sources of interpolation error for the particular case of interpolation from the analyzed field to the barometer locations. The sources of error that arise when interpolating the observations to the model grid points are similar.

Elevation reduction using equation (6) requires that we know the elevations of the barometers. We assume there is a negligible error in the elevations of the analyzed pressure fields for purposes of reduction using equation (6). However, catalogued elevations of the barometer sites can be significantly erroneous. We checked the barometer elevations by inverting equation (6) to solve for the elevation that best fit the pressure difference from the nearest model points, and we rejected those sites that differed by more than 20 m from the catalog elevation (less than 10 out of more than 400 sites were rejected). A sensitivity analysis of the error introduced by an incorrect elevation reduction indicates that a 500 m error in station elevation can increase the rms with mean removed by as much as 1.3 mbar, where a 20 m error would increase the rms by ≤ 0.02 mbar.

In addition to the elevation change, equation (6) also depends on the surface air temperature. Two different temperature fields were used for the two models: for the NCEP/NCAR data we used the model temperature at 40 m above the ground surface, whereas for ECMWF we used a 2 m air temperature (because the 40 m temperature field was not available to us on the same grid discretization as the pressure field). Note that the 40 m air temperature is more appropriate for adjustment of the surface pressure to a new elevation using equation (6) because the 2 m surface temperature is subject to noise due to boundary layer effects over continents.

We performed a sensitivity analysis to determine the error introduced by using an erroneous temperature field. We found that a bias error in temperature produces negligible change in the pressure rms, but that random errors can have a more significant effect. Random errors in the temperature field of up to 10°K will produce negligible changes in the rms of the pressure if the elevation of the measurement station is within ~ 200 m of the mean elevation of the nearest model grid points. However, when the station elevation differs by more than 200 m from the weighted mean model elevation (as commonly occurs in mountainous regions), random errors in the temperature field of the order of 1°K can influence the pressure correction significantly.

For example, the station at TMGO (Table Mountain Gravity Observatory) near Boulder, Colorado is about 500 m lower than the weighted mean of the nearest ECMWF grid points. A 1.5°K rms temperature error at those grid points would produce a 0.2 mbar rms pressure error in the interpolation of pressure to TMGO. We note that boundary layer effects can cause 2 m and 40 m estimates of air temperature to differ by as much as 1.5°K rms for the 6-hourly values. Consequently, the 6-hourly values of interpolated pressure from ECMWF and NCEP/NCAR may differ by up to a few tenths of a mbar solely because of the different temperature levels used. However, the 0.2 mbar error that might be attributed to the elevation reduction represents only about 15% of the total 1.35 mbar rms difference of the 6-hourly time series at TMGO. Consequently, most of the rms difference at TMGO consists of a real discrepancy between model and observation, and is not caused by errors in the interpolation/reduction of the model pressure to the station location. Note also that the gaussian averaged rms difference

2

between models and observations in the vicinity of TMGO (Figure 8a) is much less than 1.35 mbar; this is because the process of computing gaussian spatial averages reduces differences that are associated with pressure variations on short spatial wavelengths.

This can be seen by comparing the numbers in the columns labeled "No Spatial Averaging" in Tables 1 and 2, with those in the columns labeled "Gaussian Average".

In principle one should also consider the dependence of pressure on the specific humidity, Q, by replacing T with T(1+0.6078Q) in equation (6) [Gill, 1982]. We tested the error introduced by our implicit assumption that Q=0 and we found that the difference could introduce an error equivalent to up to 3° K rms difference in temperature. On the basis of the sensitivity analysis we performed for the temperature error, we expect that in low-relief areas the error introduced by our assumption is negligible, but in areas with high relief this error can add significantly to the pressure rms.

To further test the dependence on specific humidity, we calculated the rms difference for both the 30-day averages and the 6-hourly values for the NCEP/NCAR and the ECMWF analyzed fields. The rms difference reduced to the barometer elevations using T(1+0.6078Q) were negligibly different than those using just T in low-lying areas but in high relief regions the rms difference was actually slightly larger after correcting for Q. We attribute this to the fact that the water vapor content of the atmosphere can change significantly on scales of a few km. Hence the model discretization is too coarse to adequately constrain the water vapor content.

We also considered the effect of a variable lapse rate on interpolation using (6).

Swenson and Wahr [2000] derived an empirical linear relation between lapse rate and temperature which we used in place of the 6.5°K km⁻¹ lapse rate in equation (6). We found that it produced a negligible change in the rms values (averaging less than 0.01 mbar).

From this sensitivity analysis we conclude that the errors introduced by interpolation of the analysis field to the barometer locations are negligible. In the worst case (i.e. using 2 m air temperature for ECMWF reduction in high relief regions) the contribution to the rms difference is a few tenths of mbar, and so these errors can be neglected.

4.4. Surface pressure field from barometric measurements

An alternative means of removing the atmospheric mass contribution from the gravity field delivered by GRACE would be to use the barometric measurements themselves to estimate the large-scale pressure variations, particularly in those regions (e.g. Antarctica) where the accuracy of the analyzed pressure fields is suspect [Wahr et al., 1998]. Sufficiently dense barometric measurements could conceivably provide a more accurate estimate of the atmospheric mass contributions to GRACE in regions that are poorly constrained by global analyses.

To demonstrate the accuracy with which surface pressure fields could be reconstructed from surface pressure measurements, we created a synthetic "observed" data set by interpolating the ECMWF analyzed pressure fields to the barometer locations using the same interpolation method described previously. Then we interpolated both the original ECMWF fields and the version of ECMWF that had been interpolated

to the irregularly-spaced barometric sites on to a regular grid with elevations defined by ETOPO5 [Row et al., 1995]. We calculated the rms differences of 250-km gaussian averages of the two re-sampled data sets for both the 30-day averages and the original 6-hourly values. The rms for the 30-day averages in the United States is small, < 0.1mbar, with slightly larger values in the Rocky Mountain regions, ~ 0.3 to 0.5 mbar (Figure 9a). Even the rms differences for the 6-hourly values (Figure 9b) are small, < 0.2 mbar in flat areas, and < 0.9 in mountainous areas. Thus, even in areas where the analyzed pressure fields are known to be affected by larger errors (e.g. Antarctica), with an adequate barometer distribution it would be possible to reduce the atmospheric contamination of the GRACE hydrology estimates to values of just a few mm of water. We note however that this comparison is perhaps overly optimistic in that it assumes no gaps in the data, which would almost certainly occur to degrade the comparison. Also, if we were to instrument poorly-constrained areas of the globe, a perhaps better alternative to using the pressure measurements directly would be to let NCEP and/or ECMWF incorporate the measurements into their operational database for assimilation into the analyzed fields, and hence improve the models in those regions.

When we plot (not shown) the rms values contoured in Figures 9a and 9b as a function of the number of barometers located within the near vicinity of the point where the rms value has been calculated, we find a strong exponential relationship, with greater station density resulting in decreased rms values. We estimate that to recover the pressure field from interpolation alone with an accuracy of better than 1 mbar it is necessary to have 0.4 barometric stations per 1° x 1° area ($\approx 10,000 \text{ km}^2$), and with

Figure 9a

Figure 9b

0.8 barometers per 1° x 1° area the pressure field can be recovered with an accuracy of better than 0.5 mbar.

5. Discussion and Conclusions

The accuracy with which GRACE can map the Earth's gravity field is limited by several sources of error, including system-noise error in the satellite-to-satellite microwave ranging measurements, accelerometer error, error in the ultrastable oscillator, and orbit error. The accuracy depends somewhat on the orbital configuration (on the altitude and spacecraft separation, for example). However, system design is such that the atmospheric mass correction represents the limiting factor when using GRACE measurements to infer changes in water storage on land at wavelengths of about 300 km and larger [Wahr et al., 1998].

We expect that errors in the estimation of surface pressure result in two end-member contributions to errors in the GRACE hydrology estimates. If we assume that there is no aliasing, so that atmospheric pressure errors at periods < 60 days are nullified by GRACE averages, then we need only consider the errors in the 30-day averages of the pressure fields. This is end-member (1). The effect of aliasing from high frequency variations (semidiurnal, diurnal, and all signals with periods less than about 60 days) into the GRACE solution is more complicated. Aliasing from a short-period pressure error can affect the GRACE 30-day averages at locations well outside the region where the pressure error was located. These aliasing errors are apt to be smaller than might be inferred by just looking at the short-period pressure error, because some of that

error will indeed be averaged out over each 30-day period. But for end-member (2) we should assume, as a worst case scenario, that this averaging is totally ineffective, so that the rms error of the 6-hourly pressure fields could be fully aliased by GRACE into the 30-day hydrology estimates. This would mean that rms error > 1 mbar (as seen for example in the upper Great Lakes region of Figures 6c-6d) could introduce errors of more than 1 cm of water mass equivalent into GRACE estimates of the hydrological signal.

The largest source of uncertainty in our error estimates comes from the fact that most of the pressure observations used in our comparisons are also assimilated into the models. This has lead us to define "lower bound" and "upper bound" estimates of the error. Because of the assimilation, the results of comparisons where the analyzed fields are interpolated to the barometer locations (the "lower bound" estimate) could underestimate the true error. For that estimate we find the rms difference between the analyzed fields and the barometer measurements only at the barometer locations where data have been assimilated, and hence the rms differences do not reflect the possibility of errors in regions where there are no nearby observation points. In those "empty" regions, we might expect the analyzed pressure fields to be worse than elsewhere because there were no pressure observations to assimilate. The latter possibility motivated us to also calculate the rms difference between the analyzed fields and observations interpolated to the model grid points, where there may not be nearby measurements (the "upper bound" estimate). Interpolation of the pressure measurements to the grid points will introduce errors, even if the observations themselves are perfect, for the

reasons described in section 4.1. We expect that the errors from simple Lagrangian interpolation should be uncorrelated with the model errors, so that the variance of these new pressure differences ought to be larger than the variance of the analyzed pressure field errors alone, so long as the observed pressure values are error-free.

Errors in the pressure observations can cause our estimates to be either too large or too small, depending on the effectiveness of the assimilation. For example, suppose the barometric measurement error is large, and that the assimilation of pressure observations has little significant effect on the analyzed surface pressure fields. Then the difference between those analyzed fields and the observations will have contributions from errors in the observations, and this will cause our estimates of the errors in the analyzed fields to be inflated. On the other hand, suppose the assimilation is highly effective, so that the analyzed pressure fields are forced to agree closely with the pressure observations. This would not hurt our error estimates if the observations were error-free, since then the assimilation has simply caused the analyzed fields to be more accurate. But if there is an error in an observation, then the analyzed field would be forced towards the erroneous value at that location. That error would be common to both the analyzed field and the observation, and so would not show up in the difference. In this case, the difference would underestimate the true error in the analyzed field. Since our error estimates are already small enough to suggest that GRACE will be able to provide useful hydrological information at most locations, it is the possibility that those estimates may be too low that most concerns us here.

There are two potential contributions to observational error. One can be loosely

termed as measurement error. This includes, of course, errors in the barometric measurements themselves. Most present-day barometers provide short-term accuracies of 0.08 mbar and have long-term stabilities of 0.1 mbar per year, with overall uncertainties in the field estimated to be on the order of ±0.15 mbar [C. Conquest, personal communication]. This would cause our "upper bound" to underestimate the true upper bound by at most only 0.15 mbar. Unfortunately, there can be other forms of measurement error, including timing errors where measurements are made slightly offset to 00Z, 06Z, 12Z, or 18Z hours, but are assimilated as though they were made at exactly one of those times (e.g., surface measurements by radiosondes, which comprise 20% of our stations, are sometimes collected as much as a few hours after the targeted time if there is thunderstorm activity or equipment failure).

To independently assess the measurement error amplitude, we constructed a spatial semivariance function from the pressure measurements. The spatial semivariance is 1/2 the mean square difference between measurements as a function of spatial separation (as contrasted with the temporal semivariance used earlier for outlier removal, which is the mean square difference as a function of elapsed time). To estimate the spatial semivariance, we paired each barometric station in the U.S. with every other station, binned the station pairs according to angular distance between stations in 0.1° (~11 km) incremental bins, reduced the pressures of one station to the elevation of the other using equation (6), and summed the squared difference of all simultaneous measurements for all station pairs in the bin. The square root of the resulting estimate of semivariance is shown in Figure 10.

Figure 10

At large separations, where there is no apparent correlation between pressures at the two locations, the root-semivariance should converge to the rms of the time-variable component of surface pressure over the U.S.. In Figure 10 that large-distance limit is between 6.5 and 7 mbar. The semivariance decreases with decreasing station separation because the closer two stations are to one another, the more highly correlated their pressure records will be. Note from Figure 10 that the semivariance is approximately independent of distance for angular distances greater than about 15°. This implies that pressure variations over the U.S. are uncorrelated at angular distances of about 15° and larger.

In the limit of two stations at the same location, so that the pressure variations at those stations ought to be perfectly correlated with one another, the root-semivariance simply reflects the measurement error. Note from Figure 10 that station pairs with stations spaced less than 0.4° apart (10% of all U.S. radiosonde sites and 8% of all other U.S. barometer locations are within 0.4° of another U.S. barometer) have root-semivariance less than 0.7 mbar, and that the root-semivariance appears to intercept the y-axis (corresponding to zero station separation) at values that are no larger than a few tenths of a mbar. This suggests that measurement errors, including the timing errors from radiosondes, are indeed on the order of a few tenths of a mbar or less. Furthermore, this is an estimate of the measurement error at a single station and for a single 6-hourly value. The effects on the GRACE gaussian averages should be smaller still, and the process of taking 30-day averages should reduce them even further (compare, for example, the values shown in the "6-hourly", "No Spatial Averaging"

columns in Tables 1 and 2, with the much smaller values shown in the "30-day average", "Gaussian Average" columns).

The second potential source of error in the pressure observations is the possibility of fine-scale spatial variability in the pressure field at wavelengths shorter than can be described by either the barometer distribution or the analyzed fields. Scales this short would be finer than needed to correct GRACE data, but might still be coarse enough that a point measurement obtained with a barometer might be partially unrepresentative of the pressure field at the scale of the model grid. In this case, that short-scale pressure component would be aliased into an erroneous larger-scale pressure variation in the analyzed field that would not show up when we took the difference between the analyzed field and the observation at that location.

This possible contamination by short-scale variability caused us to consider one other approach, standard in meteorology, for estimating the absolute maximum error in the analyzed fields: comparing the barometric measurements with 6-hour forecast fields. The 6-hour forecasts use the complete set of three-dimensional analyzed fields from time t-(6 hours) as initial conditions, then propagate those fields forward to time t using the dynamical equations of the atmosphere. The input analyzed fields assimilate observations taken at time t-(6 hours). But neither they, nor the resulting forecast field, depend in any way on observations taken at time t. Thus the effects of measurement errors and of short-scale pressure variability will affect the observations at time t and the forecast fields for time t differently (assuming the short-scale variability in the observations is not significantly correlated over 6 hours), and so will not cancel when

taking the differences. This comparison will now overestimate the "true" error in the analyzed fields, both because the analyzed fields at time t are certainly improved by the assimilation of observations taken at time t, and because since the observational errors are presumably uncorrelated with the errors in the forecast fields, those observational errors will now be contributing to the differences.

For this comparison we considered only the NCEP/NCAR 6-hour forecast fields, because the ECMWF forecasts were not available to us. The map average for the comparison at the barometer locations is 0.34 mbar for the 30-day rms difference and 1.14 mbar for the 6-hourly rms difference over the U.S., and 0.34 mbar and 1.33 mbar respectively for north Africa/Arabian peninsula. In Tables 1 and 2 we also report the results of comparison at the model grid points.

Every comparison of gaussian-averaged, 30-day values shown in Tables 1 and 2 (i.e., the interpolation to either the barometer locations or the model grid points; and the comparisons with either the analyzed fields or the 6-hour forecast fields) indicates that the analyzed fields will be adequate to remove the atmospheric contribution to GRACE estimates of surface hydrological mass changes to an accuracy of better than 0.5 cm of equivalent water thickness. The comparisons of 6-hourly fields are more ambiguous, with rms values slightly smaller than 1 mbar (equivalent to 1 cm of equivalent water thickness) for most comparisons in the U.S. (excepting the comparison between barometer measurements and 6-hour forecast, which exhibits slightly larger average rms difference). Rms difference of 6-hourly fields are slightly larger than 1 mbar in north Africa/Arabia. The relevance of the 6-hourly values for GRACE, however, is

not entirely clear. Only a detailed orbital simulation can clarify the temporal-aliasing effects of the short-period atmospheric error on the GRACE mass estimates. In any case, we note that all of the results presented here are for data from 1998. The resolution of global circulation models will likely have greatly improved by the time of the GRACE launch.

The effects of fine-scale spatial variability of pressure and its impact on the analyzed pressure fields through the assimilation of observations should be investigated further, and we intend to examine this phenomenon in future work. Also, our analysis has been performed for only two regions: the United States and north Africa/Arabian peninsula. One of the reasons why this study was not conducted on a global scale is that the implications of this kind of analysis are unclear when barometric measurements are sparse or have many gaps and outliers (e.g., as was found in some portions of the north Africa/Arabian peninsula region). Nevertheless, these two regions are representative of the level of error that the analyzed field would present in most continental areas. We also conclude that previous estimates of error in the analyzed pressure fields [Wahr et al., 1998], which compared the ECMWF and NCEP pressure fields assuming that errors in the two fields were uncorrelated, significantly underestimate the true error in these fields. The errors in these two fields are in fact partially correlated.

Another conclusion of this paper is that if the distribution of barometers is sufficiently dense, then the pressure measurements can be used independently of analyzed pressure fields to correct for the effects of atmospheric mass variability. Our analysis using ECMWF pressure fields to create synthetic barometer measurements,

suggests that the U.S. barometer network would be capable of delivering 30-day gaussian-averages of surface pressure to an accuracy that is everywhere better than 0.5 mbar. This method, though, would be particularly useful for regions (e.g. Antarctica) where the analyzed fields may not currently be accurate enough to permit recovery of the desired gravity signal. The barometric network in those regions is apt to be far less complete than in the U.S.. In general, we found that with 0.4 barometers per 10,000 km² area it should be possible to obtain an accuracy of about 1 mbar. (Though we should point out that if a barometric network of this density were installed in some target region, it seems likely that even better results could be obtained by assimilating the data into the analyzed fields, rather than to rely solely on interpolation of the measurements.)

Note that our reconstruction of the pressure field from interpolated barometric measurements represents the ideal case in which the measurement time series are free from gaps and outliers. A potentially more serious problem is that when we constructed the synthetic barometric observations to derive these accuracy estimates, we ignored the possibility of pressure variability at spatial scales smaller than the 1.125° ECMWF grid spacing. Any such short-scale variability in the real pressure observations could be mistakenly aliased into the pressure fields reconstructed from those observations. This omission has motivated us to consider an entirely independent method of estimating the error in reconstructing pressure fields using observations: one in which we relied solely on our existing set of observations, rather than on the analyzed fields.

In this method, we calculated the error that would be associated with a kriging

interpolation of the barometric measurements to the model grid points. Kriging uses the semivariance properties of a field to generate the optimal interpolation [Davis,1986. The error in the interpolated values can be estimated as the dot product of the interpolation weights with the semivariance at the corresponding distances. For values of the semivariance we used the square of the smoothed root-semivariance shown as the solid line in Figure 10. The average of the kriging interpolation error in the U.S. over all measurements and at all continental grid points of the NCEP model was found to be 0.75 mbar, or better than the desired 1 mbar level of accuracy for the GRACE correction. Note that this error estimate implicitly incorporates the measurement error (including timing errors), the errors related to the aliasing of fine-scale spatial variations in pressure, and the horizontal interpolation error caused by using a linear interpolation to represent a more complicated spatial dependence. It also implicitly includes error due to the presence of gaps in the measurement time series. Furthermore, this 0.75 mbar error represents the error in the interpolated 6-hourly value at a single point. The error in 30-day gaussian averages of GRACE data will be substantially smaller.

We also considered ways in which the atmospheric correction to GRACE data might be improved, including to average the pressure field from ECMWF and NCEP/NCAR. In this way we should reduce uncorrelated errors that are present in the two fields. Comparisons of (ECMWF+NCEP/NCAR)/2 to the barometric measurements are shown in Tables 1 and 2. The improvement is very slight (0-18% improvement over the better of the two rms differences) as a consequence of the fact that most of the error in the analyzed fields is correlated.

Finally, we point out that for the purpose of this investigation, we always evaluated the spatially averaged rms error of the analyzed pressure fields, which obviously underestimates the point error at a given location. Tables 1-2 show the map average both with and without spatial averaging, and one will note that the spatial averaging improves the comparison by more than 60% with respect to the error estimation without spatial averaging.

Acknowledgments. We are very grateful to the NCAR DSS Archive, which provided all data sets used in this paper, and particularly to Dennis Joseph for help and patience while we learned how to manipulate the data sets. We thank Anthony Lowry for many helpful discussions and comments. We thank also Mariano Hortal, William Collins, Bob Kistler, Jack Woollen, Wesley Ebisuzaki, and Francois Boutier for helping to answer various questions surrounding this analysis. This research has been partially supported by NASA, under grant NAG5-7703; by the University of Texas, under contract UTA98-0205; and by CIRES, under the CIRES Innovative Research Program.

References

- Chao, B.F., and R.S. Gross, Change in the Earth's rotation and low-degree gravitational field introduced by earthquakes, *Geophys. J. R. Astron. Soc.*, 91 569-596, 1987
- Davis, J.C., Statistics and Data Analysis in Geology, Second Edition, pp.239-248, Wiley and Sons, New York, 1986.
- Dickey, J.O., et al., Satellite Gravity and the Geosphere, National Research Council Report, 112 pp., Nat. Acad. Washington, D.C., 1997.
- ECMWF, The Description of the ECMWF/WCRP Level IIIA Global Atmospheric Data Archive Data Services publication, 1995.
- Gill, A.E., Atmosphere-ocean dynamics, pp 40-41, New York, Academic Press, 1982.
- Haurwitz, B., Climatology, p 12, New York, London, McGraw-Hill Book Company, 1941.
- Jekeli, C., Alternative methods to smooth the Earth's gravity field, rep. 327, Dep. of Geod.
 Sci. and Surv., Ohio State Univ., Columbus, 1981.
- Kalnay, E., M. Kanamitsu, R. Kistler, W. Collins, D. Deaven, L. Gandin, M. Iredell, S. Saha,
 G. White, J. Woollen, Y. Zhu, M. Chelliah, W. Ebisuzaki, W. Higgins, J. Janowiak, K.
 C. Mo, C. Ropelewski, J. Wang, A. Leetmaa, R. Reynolds, R. Jenne, and D. Joseph,
 The NMC/NCAR 40-Year Reanalysis Project, Bull. Amer. Meteor. Soc., 77, 437-471,
 1996.
- Neibauer, T.M., and J.E. Faller, Continuous gravity observations using Joint Institute for Laboratory Astrophysics absolute gravimeters, *J. Geophys Res*, 97(B9), 12427-12435, 1992.
- Rocken, C., R. Ware, T. van Hove, F. Solheim, C. Alber, and J. Johnson, Sensing atmospheric water vapor with the Global Positioning System, *Geophys. Res. Lett.*, 20, 2631-2634,

1993.

- Row, L.W., Hastings, D.A., and Dunbar, P.K., TerrainBase Worldwide Digital Terrain Data
 Documentation Manual, CD-ROM Release 1.0, National Geophysical Data Center,
 Boulder, Colorado, 1995.
- Swenson, S., and J. Wahr, Estimated effects of the vertical distribution of atmospheric mass on time-variable gravity, *Submitted to J. Geophys. Res*, 2000.
- Van Dam, T., G. Blewitt, and M.B. Heflin, Atmospheric pressure loading effects on Global Positioning System coordinate determinations, J. Geophys Res, 99(B12), 23939-23950, 1994.
- Wahr, J., M. Molenaar, and F. Bryan, Time-Variability of the Earth's Gravity Field:
 Hydrological and Oceanic Effects and Their Possible Detection Using GRACE, J.
 Geophys. Res., 103, 30205-30230, 1998.
- I. Velicogna, Department of Physics and Cooperative Institute for Research in Environmental Science, Campus Box 390 University of Colorado, Boulder, CO 80309-390. (e-mail: isabella@colorado.edu)
- J. Wahr, Department of Physics and Cooperative Institute for Research in Environmental Science, Campus Box 390 University of Colorado, Boulder, CO 80309-390. (e-mail: wahr@colorado.edu)
- H.M. Van den Dool, Climate Prediction Center, National Centers for Environmental Prediction Washington DC 20233 (e-mail: hvandendool@ncep.noaa.gov)
 Received July, 2000

To appear in the Journal of Geophysical Research, ??.

This manuscript was prepared with AGU's LATEX macros v5, with the extension package 'AGU⁺⁺' by P. W. Daly, version 1.6a from 1999/05/21.

Figure 1.

Figure 3.

Figure 4.

Figure 5.

Figure 6.

Figure 7.

Figure 8.

Figure 9.

Figure 10.

Table 1.
Table 2.

Figure Captions

Figure 1. Location map depicting topography of the two studied areas: United States (a), and north Africa/Arabian peninsula (b).

Figure 2. Jekeli's gaussian weight function for radius $r_W = 250$ km: map and cross section. The cartoon depicts four observation sites below the gaussian cap. In the cross section, the gray arrows indicate the values of $W(\gamma)$ that would weight the corresponding pressure values. The weighted sum is assigned to the center of the gaussian.

Figure 3. A. Time series of surface pressure for the station south of Lake Nasser, Egypt. Gray stars represent the original time series; black circles represent the time series after outliers have been removed. B. Detail of Figure 3A.

Figure 4. A–D. Time series of surface pressure in a low relief area (Illinois): A. Observed (gray stars) and interpolated ECMWF (continuous line) surface pressure; B. Residual of ECMWF minus observed with means removed; C. Observed and interpolated NCEP/NCAR Reanalysis surface pressure; D. Residual of NCEP/NCAR minus observed with means removed. E–H. Time series of surface pressure in a high relief area (Nevada): E. Observed (gray stars) and interpolated ECMWF (continuous line) surface pressure; F. Residual of ECMWF minus observed with means removed; G. Observed and interpolated NCEP/NCAR Reanalysis surface pressure; H. Residual of NCEP/NCAR minus observed with means removed.

Figure 5. Rms difference of analyzed surface pressure field and barometric measurements for means over the 30-day averaging period, calculated at the barometer locations. Circles are barometer locations. Dashed lines are state boundaries. A. Rms difference of ECMWF and barometric measurements in the United States; B. rms difference of NCEP/NCAR Reanalysis and barometric measurements in the United States; C. rms difference of ECMWF and barometric measurements in north Africa/Arabian peninsula; D. rms difference of NCEP/NCAR Reanalysis and barometric measurements in north Africa/Arabian peninsula; D. rms difference of NCEP/NCAR Reanalysis and barometric measurements in north Africa/Arabian peninsula.

Figure 6. Rms difference of analyzed surface pressure field and barometric measurements in the United States, calculated at the analyzed grid points. A. Rms difference of ECMWF and barometric measurements for means over the 30-day averaging period; B. 6-hourly rms difference of ECMWF and barometric measurements; C. rms difference of NCEP/NCAR Reanalysis and barometric measurements for means over the 30-day averaging period; D. 6-hourly rms difference of NCEP/NCAR Reanalysis and barometric measurements.

Figure 7. Rms error of ECMWF and NCEP/NCAR Reanalysis, calculated as the difference between the two fields, divided by $\sqrt{2}$. A. Rms error for means over the 30-day averaging period in the United States; B. 6-hourly rms error in the United States; C. rms error for means over the 30-day averaging period in north Africa/Arabian peninsula; D. 6-hourly rms error in north Africa/Arabian peninsula.

Figure 8. Rms difference between analyzed surface pressure field and barometric measurements, calculated at the barometer locations. A. 6-hourly rms difference of ECMWF and barometric measurements in the United States; B. 6-hourly rms difference of NCEP/NCAR reanalysis and barometric measurements in the United States; C. 6-hourly rms difference of ECMWF and barometric measurements in north Africa/Arabian peninsula; D. 6-hourly rms difference of NCEP/NCAR reanalysis and barometric measurements in north Africa/Arabian peninsula.

Figure 9. Rms difference between the ECMWF and the synthetic "observation" datasets in the United States. A. Results for the 30-day averages; B. 6-hourly results

Figure 10. Square root of the semivariance of pressure measurements for the United States in 0.1 degree bins (gray dots) and smoothed (black line).

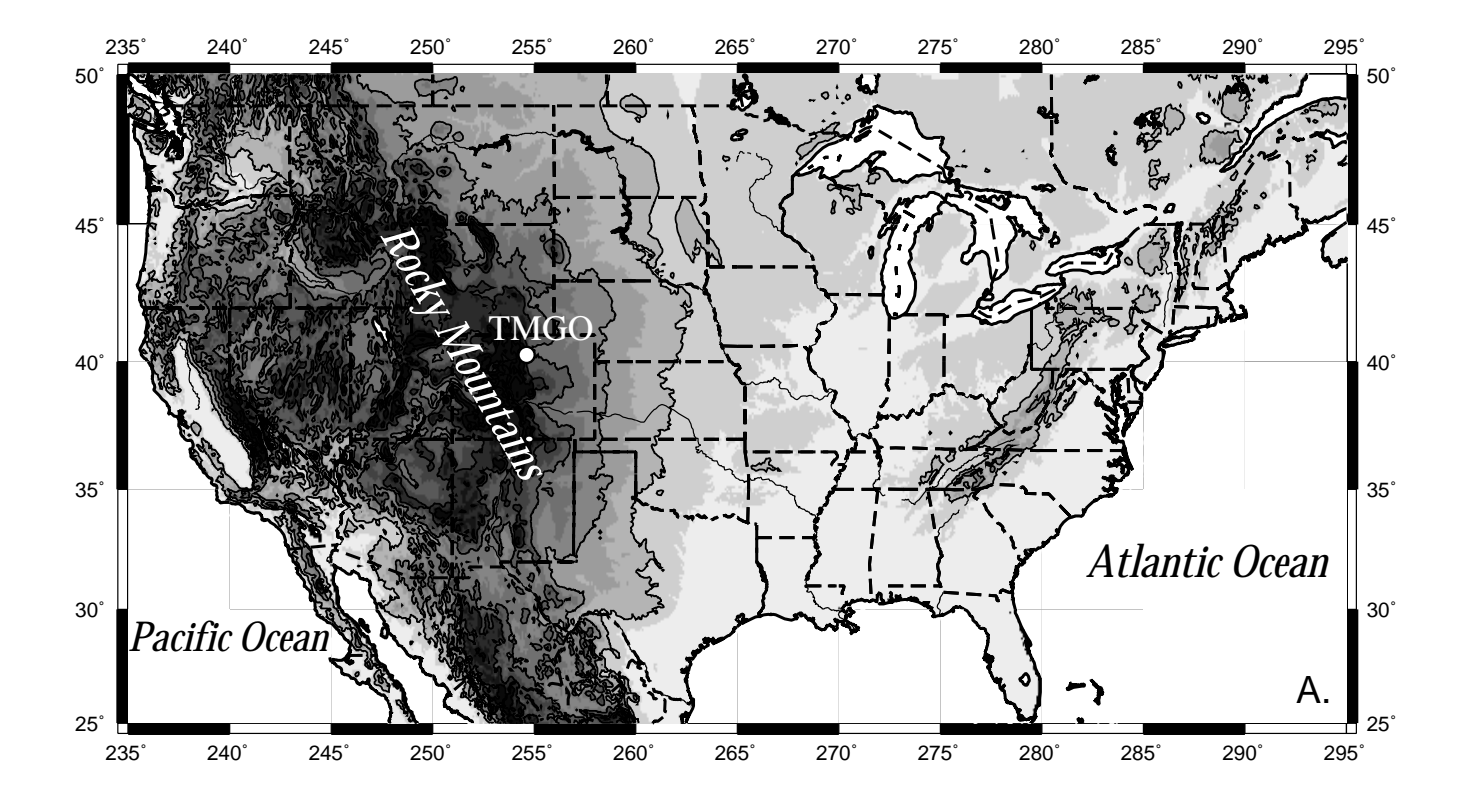
Tables

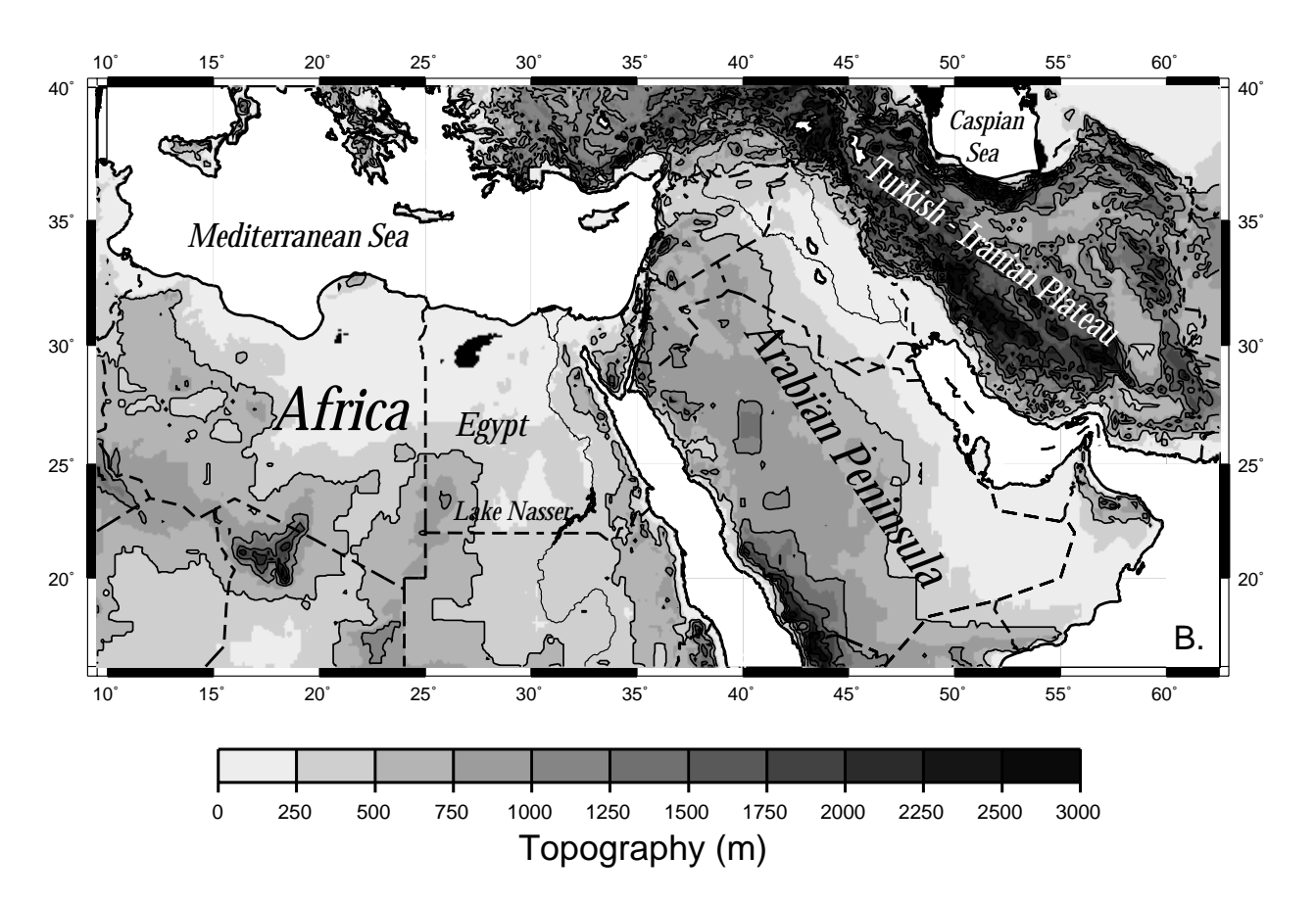
Table 1. Map averages in north Africa/Arabian Peninsula, including the rms differences (or rms error in the case of ECMWF-NCEP/NCAR) calculated with spatial averaging (equation 7, R=250 km), and without.

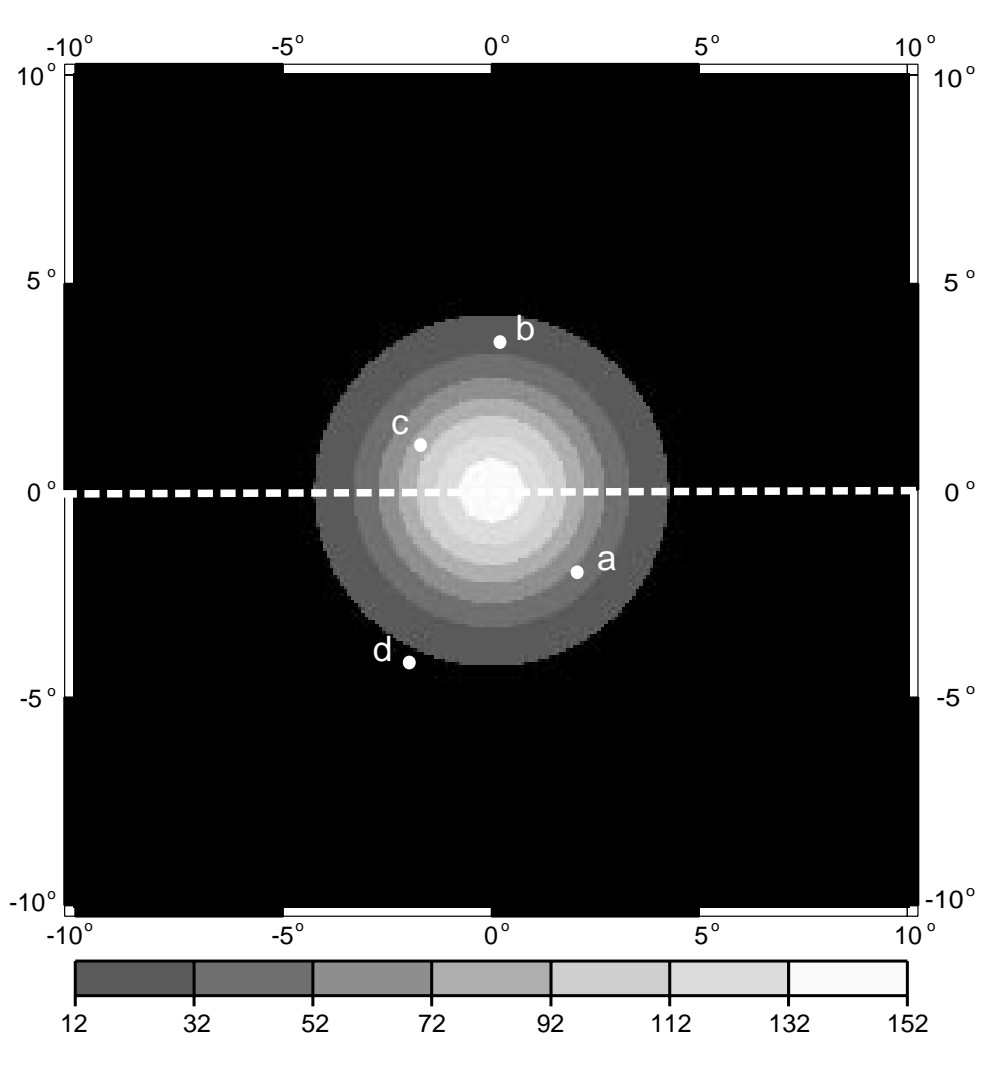
		Interpolated to barometer locations		Interpolated to model grid points	
		(mbar)		(mbar)	
		Gaussian	No Spatial	Gaussian	No Spatial
		Average	Average	Average	Average
30-day	ECMWF- obs	0.36	0.70	0.43	0.71
average	NCEP/NCAR - obs	0.26	0.62	0.48	0.63
	ECMWF - NCEP/NCAR			0.21	0.37
	NCEP/NCAR 6-hour forecast - obs	0.34	0.65	0.48	0.67
	(ECMWF + NCEP/NCAR)/2 - obs	0.26	0.59		
	ECMWF - obs	0.91	1.32	1.29	1.86
6-hourly	NCEP/NCAR - obs	0.86	1.35	1.27	1.68
	ECMWF - NCEP/NCAR			0.52	0.74
	NCEP/NCAR 6-hour forecast $-$ obs	1.33	1.70	1.61	1.98
	(ECMWF + NCEP/NCAR)/2 - obs	0.79	1.21		

Table 2. Map averages in the United States, including the rms differences (or rms error in the case of ECMWF-NCEP/NCAR) calculated with spatial averaging (equation 7, R=250 km), and without.

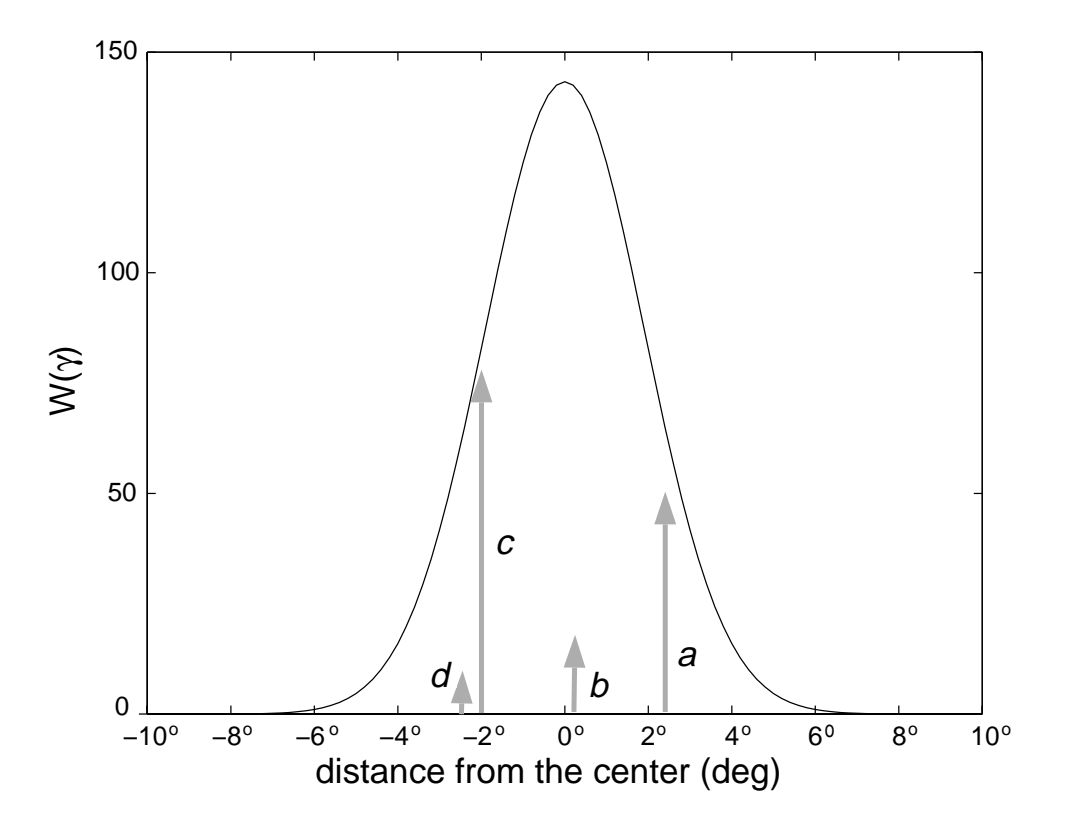
		Interpolated		Interpolated	
		to barometer locations		to model grid points	
		(mbar)		(mbar)	
		Gaussian	No Spatial	Gaussian	No Spatial
		Average	Average	Average	Average
30-day	ECMWF - obs	0.17	0.59	0.26	0.53
average	NCEP/NCAR - obs	0.16	0.64	0.23	0.45
	ECMWF -NCEP/NCAR			0.12	0.19
	NCEP/NCAR 6-hour forecast — obs	0.34	0.71	0.35	0.53
	(ECMWF + NCEP/NCAR)/2 - obs	0.13	0.58		
	ECMWF - obs	0.52	1.22	0.84	1.53
6-hourly	NCEP/NCAR - obs	0.55	1.44	0.82	1.40
	ECMWF -NCEP/NCAR			0.37	0.57
	NCEP/NCAR 6-hour forecast $-$ obs	1.14	1.79	1.29	1.77
	(ECMWF + NCEP/NCAR)/2 - obs	0.46	1.21		







Gaussian Weight Function $W(\gamma)$



0

